Mass-Spectrometry-Based Histology

DOI: 10.1002/anie.200905559

Histology by Mass Spectrometry: Label-Free Tissue Characterization Obtained from High-Accuracy Bioanalytical Imaging**

*Andreas Römpp, Sabine Guenther, Yvonne Schober, Oliver Schulz, Zoltan Takats, Wolfgang Kummer, and Bernhard Spengler**

Histological examination of biological and medical specimens has gained its universality and undisputed significance through distinct staining techniques and microscopical evaluation. Discrimination of tissue types after specific staining or labeling is an essential prerequisite for histopathological investigation, for example in accurate diagnosis of cancer. Histochemical staining techniques can only be used in a targeted manner for known compounds, and only a limited number of such targets can be visualized from a given sample at the same time. Another limitation of classical histology lies in the fact that a considerable amount of experience is required and that even well-trained pathologists often interpret histologically stained sections differently.

Mass spectrometry (MS), on the other hand, offers complex but objective and reproducible information on biological material. Imaging of biological samples by MS gained interest after development of matrix-assisted laser desorption/ionization (MALDI) as a method to desorb and ionize biomolecules, such as peptides, proteins, glycans, or lipids, with a limit of detection in the attomole range. The first proof-of-principle of imaging by MALDI was presented in 1994,[1] and was followed by numerous applications during the last decade.[2–8] An extensive overview of instrumental developments and methodological approaches in MS imaging has been published recently.[7] MS imaging allows the distribution of analytes to be investigated and displayed across a sample in a semi-quantitative manner and without the need to predefine or label selected substances prior to analysis. MALDI imaging is typically used with spatial resolutions of between 50 and 200 μm.[3] Increasing the resolution into the low-micrometer range has been demonstrated, but requires a very low limit of detection of the employed mass spectrometer, as the available amount of material per imaged spot is reduced quadratically with reduction of the spot diameter.[1,9,10]

Identification of molecules during MS imaging experiments is often limited if mass spectrometers with a rather low mass resolving power and accuracy are used. Additional off-line bulk analyses of tissue material are typically used to back up imaging results. Imaging selectivity, that is, mass bin width for allocation to image signals, is typically set to one mass unit.

Employing MS imaging for obtaining valid histological information requires a number of improvements:

1. The usable spatial resolution has to be high enough to resolve cellular features.
2. Analytical sensitivity has to be high enough to visualize the majority of interesting substances in high-lateral-resolution experiments.
3. Mass resolving power and mass accuracy have to be as high as possible when complex biological samples are under investigation. To unequivocally assign a mass signal to an image and to identify substances by accurate mass, signals have to be stable and correct in detected mass values; that is, mass accuracy should be in the low-ppm range.
4. Image assignment to mass signals has to be both highly selective and flexible. To distinguish neighboring mass signals in biological tissue samples, the coding mass bin width must typically be smaller than 0.1 mass units.
5. To clearly identify imaged substances in complex samples, MS^n data from fragmentation of precursor ions has to be obtainable directly from individual imaged sample spots.
6. Ambient pressure conditions are often necessary, rather than high-vacuum conditions, for example when working under physiological conditions, imaging volatile substances such as drug metabolites, or using volatile matrices.
7. Sample handling and preparation have to be fast and robust.
8. Results have to be achievable in a reasonable timeframe.

Some of these requirements have already been demonstrated individually. High mass resolution combined with a high spatial resolution of 7 μm was demonstrated using an ion-trap Fourier-transform ion-cyclotron-resonance mass spectrometer (IT-FTICR-MS),[9] but sensitivity was insufficient. Imaging of biological samples with FTMS was reported with a spatial resolution of only 100 μm.[5,6] A special ion source developed in our lab was used to demonstrate high lateral resolution combined with low mass resolution.[11] An alternative approach for fast and highly resolved imaging is

[*] Dr. A. Römpp, S. Guenther, Y. Schober, O. Schulz, Dr. Z. Takats, Prof. Dr. B. Spengler
Institute of Inorganic and Analytical Chemistry
Justus Liebig University Giessen
Schubertstrasse 60, Haus 16, Giessen 35392 (Germany)
Fax: (+49) 641-993-4809
E-mail: bernhard.spengler@anorg.chemie.uni-giessen.de
Homepage: http://www.uni-giessen.de/analytik
Prof. Dr. W. Kummer
Institute of Anatomy and Cell Biology
Justus Liebig University Giessen
Aulweg 123, Giessen, 35392 (Germany)

[**] Financial support by the European Union (STREP project LSHG-CT-2005-518194), by the European Research Council (ERC starting grant 2008, ZT), and by the Bundesministerium für Bildung und Forschung (BMBF, NGFN project 0313442) is gratefully acknowledged. We thank Tamara Papadakis for preparing the cryosections.

Supporting information for this article is available on the WWW under http://dx.doi.org/10.1002/anie.200905559.

mass microscopy, which comprises parallel ion-optical imaging of the complete sample area for selected mass windows. The method appears to have high potential, but is limited to date by practical constraints.[8] Secondary-ion mass spectrometry (SIMS) offers very high spatial resolution, and impressive results were reported with this technique.[12] SIMS analyses, however, are mostly limited in terms of mass accuracy at high spatial resolution, mass range, and MS/MS capability. Desorption electrospray ionization (DESI) imaging has great potential for measurements under ambient conditions, but lacks spatial resolution at the cellular level.[13]

For the first time we present herein a combination of high mass resolution and accuracy, high spatial resolution, and high analytical sensitivity to characterize and discriminate biological tissue with cellular resolution. Our atmospheric-pressure scanning microprobe matrix-assisted laser desorption/ionization mass spectrometry (AP-SMALDI-MS) setup provides a new level of information depth and quality for histological examination at the cellular level. Compounds were identified by accurate mass and product-ion analysis directly from analytical image data. Mass accuracy was typically better than 1 ppm (see also the Supporting Information).

The ion signals corresponding to phospholipid species were used to distinguish tissue types. Phospholipids are the essential building blocks of cell walls, but they also play an important role in signal transduction and are thus of biological relevance for numerous diseases. Analysis of their enzymatic degradation products, lysophosphocholins (LPCs), is demonstrated in the Supporting Information. 20 μm-thick sections of mouse urinary bladder were scanned by MS with 10 μm spatial resolution and sets of tissue-specific compounds were selected from the acquired data for imaging (Figure 1 A,B). Excellent agreement with toluidine-blue staining (Figure 1 C) was found in assigning tissue types. The outer region of the urinary bladder was characterized by the sphingomyelin compound SM(34:1) (*m/z* 741.5307; Figure 1 A, blue). This histological region could be further subdivided into the adventitial layer, the outermost thin layer indicated by increased signal intensities of SM(34:1), and the detrusor muscle mainly consisting of smooth muscle tissue.

Inside the muscle layer, the loose connective tissue of the lamina propria is located, and is characterized by intense signals of *m/z* 743.5482 (Figure 1 A, red, collocated with SM(34:1) signal in blue). Towards the bladder lumen, a thin layer of subepithelial myofibroblasts was found to be characterized again by high signal intensities from SM(34:1) (Figure 1 A, blue). The smooth muscle tissue of the detrusor muscle and the myofibroblasts showed very similar phospholipid profiles, in accordance with their similar physiological properties. The high cell densities of both layers were expressed in the stained image (Figure 1 C). The innermost layer of the mucosa is composed of the bladder epithelium (urothelium), indicated by a mass signal at *m/z* 798.5410 of the phosphatidylcholine species PC(34:1) (Figure 1 A, green).

At closer inspection the urothelium could be differentiated even further by AP-SMALDI imaging. From the basement membrane to the lumen, the urothelium is known to consist of basal cells, intermediate cells, and, facing the lumen, umbrella cells. The latter are the largest cells and cover several of the underlying cells. The reduced density of cell nuclei in this sublayer of the urothelium resulted in lighter areas in the stained image. In the AP-SMALDI image (Figure 1 B), these areas were represented by higher intensities at *m/z* 812.5566 corresponding to phosphatidylethanolamine PE(38:1) coded in green, resulting in cyan pixels by colocalization with PC(34:1) coded in blue. Blood vessels

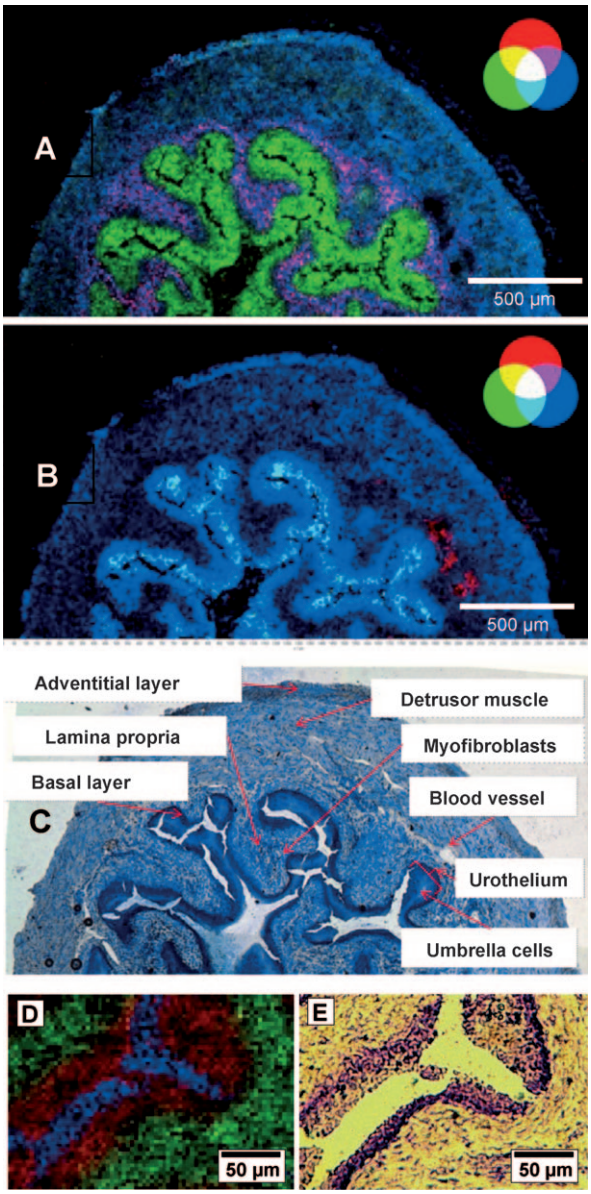

Figure 1. Mouse urinary bladder: A) 10 μm step size, overlay of ion images for *m/z* 741.5307 (blue, muscle tissue, SM(34:1)), *m/z* 798.5410 (green, urothelium, PC(34:1)), and *m/z* 743.5482 (red, lamina propria). B) Overlay of ion images for *m/z* 798.5410 (blue, urothelium, PC(34:1)), *m/z* = 812.5566 (green, umbrella cells, PE-(38:1)), and *m/z* 616.1767 (red, blood vessels, heme b, M^+). C) Optical image of the same tissue section after staining with toluidine blue. D) 5 μm step size, overlay of ion images for *m/z* 114.9039 (In^+ substrate, blue), *m/z* 798.5410 (PC(34:1), red), and *m/z* 741.5307 (green). E) Optical image of the same tissue section after staining with toluidine blue. All of the ions are of type $[M+K]^+$ except for heme.

were detected, based on imaging of the heme signal at m/z 616.1767 from residual blood (Figure 1B, red). Again, these features correlate exactly with information from toluidine-blue staining. The various tissue types are identifiable after histological staining by a trained pathologist. By MS imaging, even those regions that are hardly expressed by classical histological examination are clearly discriminated (Figure 1A,B).

In another experiment, spatial resolution was further increased to closer investigate regions of interest. Figure 1D shows an AP-SMALDI image of an area of the urinary bladder with two different, adjacent tissue types; the image was acquired with a step size and ablation spot size of 5 μm. Ion distributions again correlated well with histological features indicated in the stained-tissue image (Figure 1E). The AP-SMALDI image provides pixel-sharp separation between the muscular layer (m/z 741.5307, green) and the urothelium (m/z 798.5410, red) with no blur or signal overlap (yellow pixels), which demonstrates that the effective analytical resolution is indeed in the range of 5 μm.

High mass accuracy is of great advantage for immediate identification of compounds in tissue. The instrument provides a mass accuracy of 2 ppm after external calibration. Furthermore, each spectrum was individually calibrated using so-called lock masses to fine-tune spectra according to detected mass values of known peaks.[14] Mass accuracy achieved with this method was better than 1 ppm for all identified compounds.

A spectrum from the urinary bladder imaging experiments is shown in Figure 2A. Accurate mass values can be used to directly assign mass signals to certain compound classes such as lipids, peptides or matrix compounds.[15] Discrimination of matrix-related signals and analyte signals was possible based on mass-defect evaluation. In Figure 2A, all phospholipid signals have m/z values with decimal places around 0.5. Matrix-related signals on the other hand are found at 716.1246 and at 852.1407. Mass-based classification is especially useful when identifying unknown compounds in a mass range in which matrix-related signals are abundant. In complex samples, such as tissue sections, high mass accuracy is advantageously employed to directly identify individual analytes from a single imaging spot.

Substance identification and characterization can be further improved by MS/MS fragment-ion analysis (see the Supporting Information). Fragment ions provide information on phospholipid head groups. A PC structure was identified from product ion m/z 713.4518 after loss of $N(CH_3)_3$ from the choline headgroup. It must be noted that structural isomers of the acyl chains cannot always be differentiated even by combining MS/MS analysis and accurate mass.

Using dedicated imaging software, high mass accuracy and resolution was preserved when selecting mass spectral images. All images were generated using a highly discriminatory m/z bin width, $\Delta m/z = 0.01$, for image assignment, which was necessary to distinguish compounds which were significant for structural contrast but were close in m/z. In Figure 2B, spatial distributions of two compounds that differ in mass by only 0.05 are shown. The signal at m/z 770.5097 (green) corresponds to the K^+ adduct of PC(32:1), predominately present in the epithelium of the urinary bladder. The neighboring signal at m/z 770.5698 (isotopologue of the K^+ adduct of SM(36:1)) shows a complementary spatial distribution with high intensities in the muscle and connective tissue. Selectivities of reported MALDI images were typically limited to $\Delta m/z$ 1 (MALDI-TOF) or $\Delta m/z$ 0.1 (FTICR[5]) to date. These settings are insufficient to detect fine differences, such as those described above, that are typical for real biological problems.

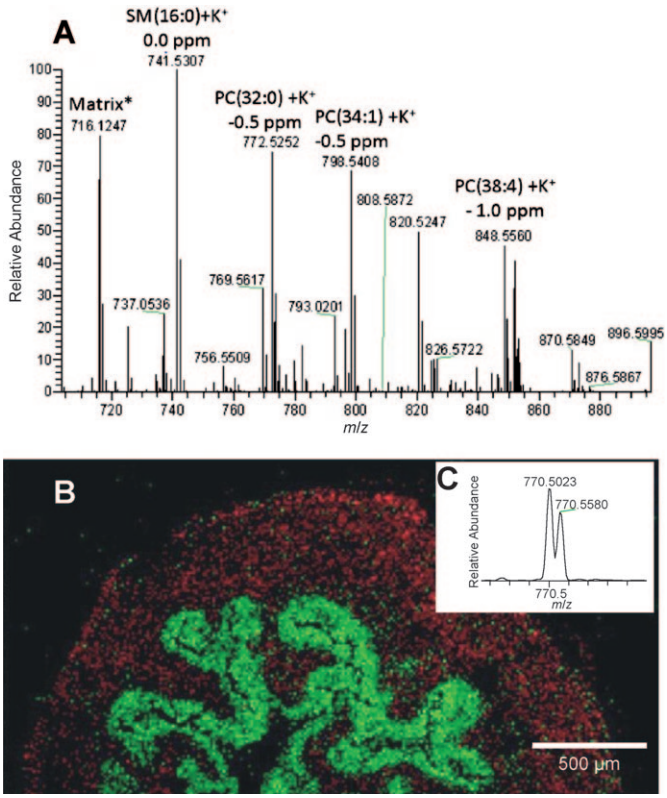

Figure 2. A) Orbitrap full-scan spectrum, Averaged, after recalibration. B) Overlay of ion images: m/z 770.5097 (red) and m/z 770.5580 (green). C) Averaged orbitrap spectrum showing both separated peaks.

A biomedical application of our new technique is illustrated by analyzing human tissue sections of infiltrating ductal carcinoma, the most abundant and also most dangerous type of breast cancer.[16] As the malignant proliferation usually infiltrates surrounding adipose tissues, the histological investigation of intraoperatively collected fresh frozen samples is not straightforward owing to undesirable characteristics of adipose tissue. Whilst classic histology provides ambiguous results, AP-SMALDI imaging of these tumors resulted in distinction of tumor and surrounding healthy tissues. Ductal carcinoma samples were found to contain characteristic lipid constituents such as various gangliosides.[17] Specific lipid profiles could provide unequivocal identification of cancer cells by MS imaging. In Figure 3, a thin section of infiltrating ductal carcinoma is shown with clear distinction of cancerous (red) and healthy (green) tissue at 10 μm spatial resolution.

Another important application of high-resolution MS imaging is the detection of neuropeptides, which can act as

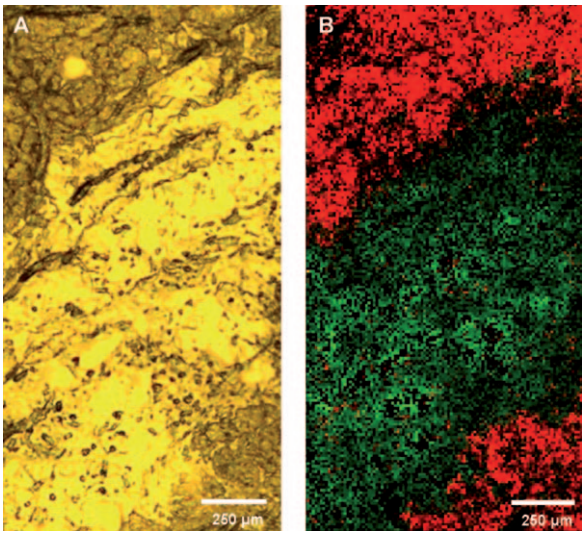

Figure 3. Human ductal carcinoma. A) Optical image of a tissue section. Darker areas indicate tumor tissue. B) 10 µm step size, overlay of ion images for *m/z* 529.3998 (healthy, green), *m/z* 896.6006 (tumor, red, PC(34:1), $[M+K+DHB-H_2O]^+$).

marker compounds for a large number of diseases and physiological processes.[18] Mouse pituitary gland was imaged at 10 µm spatial resolution (Figure 4A). The posterior and the anterior lobe are clearly distinguished based on phospholipid signals at *m/z* 826.5723 (PC(36:1), green) and *m/z* 848.5566 (PC(38:4), blue). These features again correlate exactly with the staining experiment (Figure 4B). The neuropeptide vasopressin at *m/z* 1084.4451 is coded in red (Figure 4A). It is located in the central part of the posterior lobe, corresponding to its biological function. A full-scan mass spectrum from an individual 10 µm pixel is shown in Figure 4C.

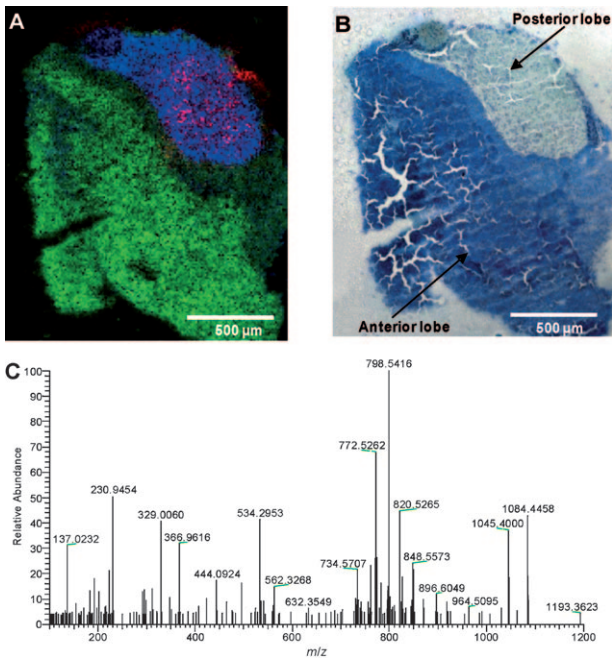

Figure 4. Neuropeptide in mouse pituitary gland: A) 10 µm step size, overlay of ion images: $[M+H]^+$ of vasopressin (*m/z* 1084.4451, red), PC(36:1) (*m/z* 826.5723, green, $[M+K]^+$), and PC(38:4) (*m/z* 848.5566, blue, $[M+K]^+$). B) Optical image after toluidine-blue staining. C) Full-scan spectrum of an individual 10 µm pixel.

The current setup includes a few principle limitations that have to be overcome in the future. MALDI-based mass spectrometric imaging requires application of a suitable matrix layer, introducing the risk of artifact formation and a crystal-size-related resolution limit. The mass range of $m/z < 4000$ is another limit of the current instrumentation, making direct protein detection impossible. Accurate mass and MS/MS are very helpful for identification of imaged compounds, but do not always provide a complete structural characterization (namely in terms of fatty acid isomer analysis). Our results, however, show that biologically relevant and highly specific information can be derived from AP-SMALDI images with µm spatial resolution. They are a distinct methodological improvement for biological applications, for the first time combining high spatial resolution, high mass accuracy, and high sensitivity. For histological investigation, the method provides an unprecedented quality and reliability of information on chemical content. With that, it has the potential to supplement classical histological protocols and support histopathology by adding another dimension of diagnostic information on the molecular level.

It is important to note that pathologically relevant information in MS imaging is obtained from untargeted experiments, meaning that structure-specific substances do not have to be selected or identified beforehand but can be discovered as specific markers during image analysis. Pathologically alerting structures may thus be found even if marker biochemistry, for example of a carcinoma type, is not yet identified, which is a major advantage over histochemical staining. Another advantage of AP-SMALDI imaging-based histology is that interpretation of results can become operator-independent and impartial once a standard measurement procedure has been established, because structure-defining signal patterns can be automatically identified and quantified.

Experimental Section

All the experiments were performed with a AP-SMALDI imaging source built by us.[9] The laser was focused by a centrally bored objective lens to a diameter of 5 to 10 µm. Controller software and hardware for the scanning procedure were developed in-house. The imaging source was attached to a linear ion trap/Fourier transform orbital trapping MS (LTQ Orbitrap Discovery, Thermo Scientific GmbH, Bremen, Germany) with a mass resolving power of 30000 at *m/z* 400 in positive-ion mode. This setup offers atmospheric pressure compatibility, MS^n capability, and sub-ppm mass accuracy. A UV laser with a repetition rate of 60 Hz (LTB MNL-106, LTB, Berlin, Germany) was used for desorption/ionization. Cycle times of the ion trap/orbitrap system were 1.3 seconds (including stage movement). The mass range was *m/z* 100–1000 for measurements of phospholipids and *m/z* 100–1200 for the detection of peptides. Samples were coated with DHB (2,5-dihydroxybenzoic acid) matrix using a pneumatic sprayer. Assignments of lipids were confirmed by MS/MS analysis directly from tissue (isolation window $\Delta m/z$ 3). All images were generated with a bin width of $\Delta m/z$ 0.01. More details are given in the Supporting Information.

Received: October 5, 2009
Revised: January 26, 2010
Published online: April 15, 2010

Keywords: accurate mass · histology · imaging · mass spectrometry · spatial resolution

[1] B. Spengler, M. Hubert, R. Kaufmann in *Proceedings of the 42nd Annual Conference on Mass Spectrometry and Allied Topics*, Chicago, Illinois, **1994**, p. 1041.
[2] M. Stoeckli, P. Chaurand, D. E. Hallahan, R. M. Caprioli, *Nat. Med.* **2001**, *7*, 493.
[3] F. Benabdellah, D. Touboul, A. Brunelle, O. Laprevote, *Anal. Chem.* **2009**, *81*, 5557.
[4] M. Stoeckli, D. Staab, A. Schweitzer, *Int. J. Mass Spectrom.* **2007**, *260*, 195.
[5] I. M. Taban, A. F. M. Altelaar, Y. E. M. Van der Burgt, L. A. McDonnell, R. M. A. Heeren, J. Fuchser, G. Baykut, *J. Am. Soc. Mass Spectrom.* **2007**, *18*, 145.
[6] R. R. Landgraf, M. C. P. Conaway, T. J. Garrett, P. W. Stacpoole, R. A. Yost, *Anal. Chem.* **2009**, *81*, 8488.
[7] L. A. McDonnell, R. M. A. Heeren, *Mass Spectrom. Rev.* **2007**, *26*, 606.
[8] L. A. Klerk, A. F. M. Altelaar, M. Froesch, L. A. McDonnell, R. M. A. Heeren, *Int. J. Mass Spectrom.* **2009**, *285*, 19.
[9] M. Koestler, D. Kirsch, A. Hester, A. Leisner, S. Guenther, B. Spengler, *Rapid Commun. Mass Spectrom.* **2008**, *22*, 3275.
[10] B. Spengler, M. Hubert, *J. Am. Soc. Mass Spectrom.* **2002**, *13*, 735.
[11] P. Chaurand, K. E. Schriver, R. M. Caprioli, *J. Mass Spectrom.* **2007**, *42*, 476.
[12] S. G. Ostrowski, C. T. Van Bell, N. Winograd, A. G. Ewing, *Science* **2004**, *305*, 71.
[13] J. M. Wiseman, D. R. Ifa, Q. Song, R. G. Cooks, *Angew. Chem.* **2006**, *118*, 7346; *Angew. Chem. Int. Ed.* **2006**, *45*, 7188.
[14] B. Spengler, *J. Am. Soc. Mass Spectrom.* **2004**, *15*, 703.
[15] B. Spengler, A. Hester, *J. Am. Soc. Mass Spectrom.* **2008**, *19*, 1808.
[16] Interpretation of breast biopsies, 4th ed., Raven Press, New York, **2002**.
[17] G. Marquina, H. Waki, L. E. Fernandez, K. Kon, A. Carr, O. Valiente, R. Perez, S. Ando, *Cancer Res.* **1996**, *56*, 5165.
[18] L. J. Li, J. V. Sweedler, *Annu. Rev. Anal. Chem.* **2008**, *1*, 451.

